Controlled Potential Coulometry for the accurate determination of plutonium in the presence of uranium: The role of sulfate complexation

Giacomo Canciani, Ygor Davrain, Marielle Crozet, Danièle Roudil, Sébastien Picart

Controlled Potential Coulometry for the Accurate Determination of Plutonium in the Presence of Uranium: the Role of Sulfate Complexation

Giacomo Canciani [a], Ygor Davrain [a], Marielle Crozet[a], Danièle Roudil[a], and Sébastien Picart [a*]*

[*] ***Corresponding Authors:*** *E- mail: Giacomo.Canciani@cea.fr (G.Canciani), Sebastien.Picart@cea.fr (S. Picart)*

[a] *CEA, DES, ISEC, DMRC, CETAMA, Univ Montpellier, Marcoule, France*

E-mails : Ygor.Davrain@cea.fr (Y.Davrain), Marielle.Crozet@cea.fr (M.Crozet), Danielle.Roudil@cea.fr (D.Roudil)

Keywords: Controlled-potential coulometry, Plutonium, Sulfate, Uranium, Complexation, Speciation

Abstract

Controlled Potential Coulometry (CPC) is generally regarded as one of the most accurate analytical methods available for the quantification of plutonium (Pu) in acidic aqueous solutions. With a growing use of mixed oxide nuclear fuel, there has been an interest in the technique's applicability to the analysis of Pu in the presence of uranium (U). Expanding on previous studies, the work presented herein demonstrates the highly accurate CPC analysis of Pu in mixed solutions (Pu + U) containing large quantities of U (U:Pu up to 100:1) as well as establishing the role played by sulfate anions during the analyses.

By combining experimental results with speciation simulations, it is shown that the introduction of U in mixed Pu + U solutions is accompanied by increases in sulfate ions in the nitric acid medium which complex unequally with the different Pu cations in solution. The anions' stronger affinity of for Pu(IV) rather than Pu(III) causes a decrease in the formal potential of the Pu(IV)/Pu(III) redox couple, directly affecting the degree of completion of the electrochemical reactions performed during CPC. A correction factor, f, is applied to account for the degree of completion of the analysis' electrochemical steps and compensate for the effects of complexation. Thereby, a level of accuracy comparable to that achieved during the analysis of pure Pu solutions, is attained.

Ultimately, a series of recommendations are put forward such that it becomes possible to maintain CPC's good analytical performance for the measurement of Pu content in mixed Pu + U solutions.

Introduction

As society approaches the cusp of an energetic revolution, the profile of global energy production is expected to undergo radical change in the first half of the 21st century as a response to the decarbonisation required to mitigate climate change. In this context, the global production of electricity from nuclear energy is expected to rise by 27 – 62 % by 2040 [1]. For the nuclear field, this increase highlights the importance of resource optimisation with the development of spent fuel reprocessing and plutonium recycling becoming essential in order to ensure a reliable supply of fissile

materials [2,3]. With that in mind, the development of analytical methods for the accurate determination of actinides (primarily uranium (U) and plutonium (Pu) isotopes) remains essential not only in an industrial context but also for purposes of non-proliferation and international safeguards. In order to achieve high degrees of accuracy as well as to calibrate and validate their analytical methods and equipment, companies and institutions working in the field rely on the use of Certified Reference Materials (CRMs) [4–6]. One of the main missions of the French alternative energies and atomic energy commission (CEA)'s Committee for the Establishment of Analysis Methods (CETAMA) is to develop and provide CRMs for nuclear analysis laboratories worldwide [4,7–9]. The production of such reference materials requires the use of highly accurate elemental analysis methods, which vary according to the elements present in the produced CRM [10].

In the case of plutonium analysis, three techniques are routinely used to achieve the required high levels of accuracy during the production of CRMs: redox titrimetry, Isotope Dilution Thermo-Ionisation Mass Spectrometry (ID-TIMS), and Controlled Potential Coulometry (CPC). Of the three techniques, CPC is the most accurate, achieving particularly low measurement uncertainties (0.1% for samples containing 4 – 15 mg of Pu [11,12]), whilst redox titrimetry and ID-TIMS have higher uncertainties of 0.17 – 0.28 % [13] (for samples containing 5 – 60 mg of Pu), and 0.21 – 0.28% [10] (for samples containing 10 – 50 ng of Pu), respectively. The good analytical performance of CPC arises from its underlying principles, as discussed below.

CPC enables the determination of the content of an electroactive species in solution by studying the quantity of charge required for the studied species to undergo an electrochemical transformation. CPC is based on Faraday's law where the mass, m, of an element is related to the molar mass of the studied species, M, the number of electrons exchanged during the electrochemical transformation of the species, n, Faraday's constant, F, (equal to 96485.33212 C/mol [14]) and the quantity of electrical charge involved in the studied reaction, Q, as shown in equation (1). Q is usually determined by integrating the amount of current used over the time of analysis. It can thus be seen that, unlike other analytical techniques, CPC is based on physical (time and current) rather than chemical parameters. This traceability to more accurate physical standards renders CPC an absolute technique and results in excellent degrees of trueness and precision [15].

$$m = \frac{Q\,M}{n\,F} \qquad (1)$$

With a rise in the recycling of spent nuclear fission fuel through mixed uranium/plutonium oxide (MOX) fuels [2], there has been an increased demand for mixed actinide CRMs. As a response, in April 2018 the CETAMA produced the EQRAIN (U + Pu) n°02 mixed oxide CRM. In light of the importance of mixed U + Pu CRMs as well as the recent production of EQRAIN (U + Pu) n°02, there has been a growing interest in expanding the analytical applications of CPC analysis for Pu content from pure Pu solutions to mixed Pu and U (i.e. Pu + U) solutions.

CPC is a particularly interesting technique for the analysis of Pu content in mixed Pu + U CRMs since – beyond its particularly high degree of accuracy – it allows the direct analysis of Pu in mixed Pu + U solutions without separation procedures (which, for example, are imperative for ID-TIMS analyses). This advantage arises due to the large difference between the redox potentials of the Pu(IV)/Pu(III) and the U(VI)/U(IV) redox pair in aqueous nitric acid (HNO_3) media [16], meaning that the determination of Pu through CPC can be performed without significant interferences from U

[11,12,17]. This lack of interference from the U ions can be attributed to the stability of U in the (VI) valence state as UO_2^{2+} in the aqueous acidic analysis conditions[18].

The CPC analysis of Pu in the presence of U in aqueous acidic solutions has been previously studied through two main perspectives. Firstly, the effect of U on the accuracy of the analysis was investigated in the general context of the effects of various metallic impurities [17,19–21]. During these studies it was ascertained that the presence of U did not interfere significantly with the coulometric determination of the Pu content of a solution (for U:Pu mass ratios ≤ 58:1). The second aspect has been the development of a technique for the determination of Pu through the joint analysis of Pu and U in mixed Pu + U solutions [22–25]. Unfortunately, these techniques resulted in both an increase in experimental complexity and a decrease in the analytical accuracy for the analysis of Pu content (arising from the correction required to isolate the electrochemical response of Pu from that of U). Furthermore, in both series of studies the CPC analysis of Pu was performed in sub-optimal experimental conditions; namely the use of platinum (Pt) working electrodes (which display a limited electrochemical window due to their propensity for generating surface adsorbed hydrogen [26]) and sulphuric acid (H_2SO_4) or perchloric acid ($HClO_4$) electrolytes (which present significant disposal problems in nuclear environments).

At the CETAMA's metrological laboratory for nuclear matter (LAMMAN), the use of CPC for the determination of the Pu content of U + Pu CRMs in HNO_3 electrolytes (selected as the optimal medium in terms of precision in reproducibility conditions and effluent management) has been the subject of preliminary studies by *Ruas et al.* [11]. In their study, the applicability of CPC to solutions of Pu + U (with mass ratios U:Pu up to 10:1) with a gold (Au) working electrode (known to show an improved stability in nitric acid and provide better analytical results for CPC than the traditionally used Pt [27]) was evaluated.

They showed that, whilst the coulometric analysis of Pu could be performed with an acceptable degree of accuracy, increasing concentrations of U in solution resulted in a cathodic shift in the formal potential of the Pu(IV)/Pu(III) redox couple. It was postulated by *Ruas et al.*[11], in accordance with the observations previously made by Shults [17], that these shifts could be attributed to an increase in sulfate (SO_4^{2-}) concentration in the systems. However, a quantitative analysis of the role played by sulfate anions in the observed shifts was not performed during either study. Furthermore, the works of Ruas *et al.* and Shults were limited to studying U:Pu ratios of 60 and 10, respectively; these ratios are significantly smaller than those encountered in the spent fuel reprocessing cycle [28].

The work presented in this paper expands from the preliminary studies presented by Ruas through two main axes of research. Firstly, through the use of electrochemical experiments in combination with speciation simulations, we elucidate the role played by the sulfate anions in the studied solutions, their precise origin, and how their complexation with Pu cations present in the solution can lead to the observed interferences. Secondly, the present work aims to fully demonstrate the applicability of CPC as a metrological technique for the analysis of Pu + U CRMs through a performance study on a Pu + U CRM provided by the CETAMA, as well as showing the technique's applicability to solutions with large quantities of U relative to Pu (U:Pu up to 95.6:1) .

Finally, by combining the understanding gained from the speciation simulations with the results of the CPC analyses, the authors of this paper provide recommendations for the accurate analyses of Pu in mixed Pu + U CRM solutions wherein U:Pu ≤ 96.

Experimental Methods

In the present work, three different types of solutions were studied: Pu solutions (experiment YD 60), Pu solutions spiked with H_2SO_4 (experiments YD 61-63), and Pu +U solutions (experiments 48-59). In order to yield statistically significant results, multiple experiments were performed for the Pu samples spiked with H_2SO_4 as well as the for Pu + U samples. The concentrations of the chemical species in the analysed solutions were the same within each series of repetitions.

1 - Chemicals

During the study, analytical grade chemicals – concentrated HNO_3 (Merck, 68% ultrapur), concentrated H_2SO_4 (Merck, 95-97% for analysis), sulfamic acid ($HOSO_2NH_2$, Merck, Emsure, ≥ 99.0%), and hydrogen peroxide (H_2O_2, Merck, 30% v/v) – were purchased from VWR.

The pure Pu solutions studied (experiments YD 60, YD 61, YD 62, and YD 63) were prepared by diluting an aliquot of standard solution (EQRAIN Pu n°14) of Pu nitrate supplied by the CETAMA's LAMMAN (Vial # S028) in HNO_3 (0.9 mol L^{-1}). The standard solution used is traceable to the MP2 Pu metal CRM. The reference Pu content of the standard solution was established as (5.5326 ± 0.0066) g kg^{-1} (with a coverage factor of k=2) on the date of fabrication (20/03/2017). The density of the reference solution is (1.14464 ± 0.00012) at 20 °C (k=2). The molar mass of Pu in the solution on the date of analysis was determined considering both the MP2 isotopy and the decay of the Pu isotopes. As such, the molar mass and content of Pu were determined to be (239.07453 ± 0.00010) g mol^{-1} (k=2) and (5.5322 ± 0.0066) g kg^{-1} (k=2) on the 26/03/2019.

The mixed Pu + U solutions analysed during the study (experiments YD 48 -59) were directly sampled from a standard solution (EQRAIN (U + Pu) n°02) of Pu nitrate and uranyl nitrate supplied by the CETAMA's LAMMAN (Vials # S061, # S074,and # S089) in HNO_3 (0.9 mol L^{-1}). The Pu in the standard solutions used is traceable to the CETAMA's MP2 Pu metal CRM whilst the U is traceable to the CETAMA's MU 2 metal CRM. The reference Pu content of the standard solutions was determined to be (1.1192 ± 0.0013) g kg^{-1} (k=2) on the date of fabrication (26/04/2018). The reference U content of the standard solution was determined to be (106.52 ± 0.13) g kg^{-1} (k=2). The density of the reference solution is (1.26857 ± 0.00012) g mL^{-1} at 20 °C (k=2). The content of Pu in the solution on the date of analysis was determined by taking into account the MP2 isotopy and the decay of the Pu isotope, as previously done for the Pu nitrate standard solution and did not change significantly.

2 – Electrochemical apparatus

All of the electrochemical analyses (cyclic voltammetry, CPC, and the determination of formal redox potentials through coulograms) performed during this series of experiments, used the same set-up (shown in figure 1). The electrochemical cell consisted of a three-electrode system (EG&G model 377A coulometry cell system) composed of a cylindrical (diameter 3.5 cm, height 2 cm) Au working electrode (99.99% pure, manufactured by Heraeus, Germany) with a large surface area (four layers of 100 mesh/cm^2 grid, with a surface of (123 ± 5) cm^2) (k=2), a saturated calomel reference electrode (SCE, EG&G model K007) and a Pt mesh counter electrode (CE).

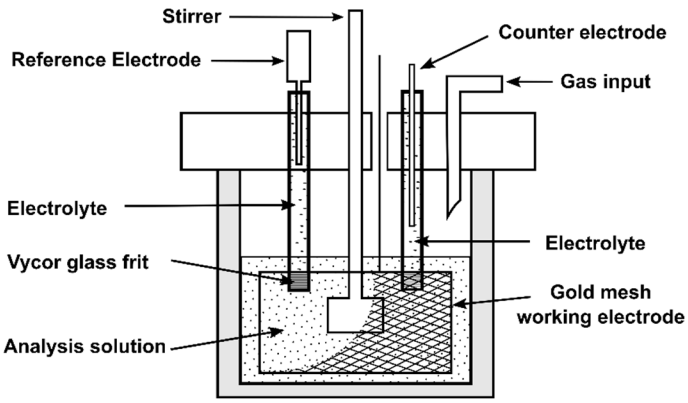

Figure 1: *Experimental set-up used for the coulometric experiments.*

The CE and SCE were placed in individual electrolytic compartments filled with the same electrolyte used in the main compartment (HNO_3, 0.9 mol L^{-1}). Vycor glass frit membranes were used to establish an electrolytic junction with ultra-low leakage rates between the secondary cells and the main compartment of the analysis cell. The separation of the SCE and CE from the analysed solutions limits the transport of products between the working electrode and the CE as well as minimising any contamination of the analysed solutions by the filling solution of the SCE.

In order to remove oxygen from the system, a constant flow of argon was maintained over the surface of the studied solutions. The flow of inert gas was humidified by a bubbler containing de-ionised water placed upstream from the electrochemical cell in order to prevent the bulk solutions from drying out. No significant cooling effects on the studied solutions were observed from this gas flow.

Finally, a paddle type stirrer (EG&G model 377 synchronous stirring motor) made of glass (with a geometry optimised in order to avoid splashing of the solution) was used for the coulometry and coulogram experiments.

The electrical components used in combination with the electrolytic cell varied according to the experiments performed:

- Cyclic voltammetry experiments were performed by using a PARSTAT 3000A Potentiostat from AMETEK scientific instruments in combination with the supplied “Versastudio” Software (version 2.60.6).

- CPC and coulogram experiments were carried out using a PAR 263A potentiostat coupled with a high precision current integrator (previously described by RUAS *et al.* [11]). The PAR 263A was controlled through an in-house software, which also allowed for the collection and analysis of experimental data.

3 – Experimental procedures

Sample preparation

The Pu standard solution (containing about 5.5 g kg^{-1} of Pu) was diluted by weight in HNO_3 (0.9 mol L^{-1}) with a dilution factor close to four before sampling into four aliquots, ensuring that each aliquot

(4 mL volume) weighed more than 1 g and contained a mass of Pu greater than 1 mg (about 6 mg per sample). This limits the relative weighing error and enables the measurement of an optimal quantity of electrical charge, as previously described by Picart *et al.* [15]*)*. As the concentration of Pu in the mixed Pu + U solutions is much lower (1.1 g kg^{-1}) than that of the Pu standard, the mixed standard solutions were used as received without dilution and divided into four aliquots of 4 mL.

In all cases, the samples were weighed directly into the coulometric glass cells used for CPC analysis, and the measurements performed with the analytical scales were corrected for air buoyancy in order to eliminate systematic errors.

Once the aliquots had been transferred and weighed, H_2SO_4 (1 mL, 3 mol L^{-1}) was added to the analysis cells in order to stabilize the actinides as Pu(IV) disulfate and uranyl (VI) sulfate crystals during the fuming procedure. A few drops of H_2O_2 (30% v/v) were further added to the solutions to reduce any Pu(VI) present to Pu(III) which , upon gentle heating is oxidised by the nitrate ions in solution to Pu(IV) [29–31]. The created solutions were left to homogenise and react overnight prior to fuming to dryness under a nitrogen sweep. Upon drying, any chloride, fluoride, and volatile organic compound impurities are eliminated. The presence of H_2SO_4 in the fumed solutions prevents the formation of insoluble oxides by stabilising the Pu and U as soluble sulfate crystals.

To perform the electrochemical analyses, the solids created from the drying procedure were redissolved in an electrolyte composed of 30 mL of HNO_3 (0.9 mol L^{-1}) with a two drops (approx. 100 µL) of sulfamic acid (1.5 mol L^{-1} in de-ionised water).

In order to study the potential interferences on the analyses caused by the presence of SO_4^{2-} anions, pure Pu standard solutions were spiked with H_2SO_4 after fuming. For these samples, 200 µL of H_2SO_4 (3 mol L^{-1}) was added to each of three analytical bulk solutions (YD 61, YD 62, and YD 63) prepared from the Pu standard solution prior to performing electrochemical analysis experiments.

Coulometric analysis

The analysis of the Pu content of solutions was performed through a four-step procedure:

1) Electrical calibration

   The analog-to-digital converter used to digitize the current measured during the CPC and coulogram experiments was calibrated with a high-accuracy current calibrator (AOIP, SN 8310). The appropriate corrections were then automatically applied to the current measurements performed during CPC and coulogram experiments.

2) Electrode pre-treatment

   Prior to analysis, the Au working electrode was electrochemically cleaned through a pre-treatment procedure in HNO_3 (0.9 mol L^{-1}) with two drops (approx. 100 µL) of sulfamic acid (1.5 mol L^{-1}). Sulfamic acid was added to the solution as a non-electrochemically active inhibitor for any nitrous acid generated by HNO_3 reduction at the electrode, as previously described in literature [11,31,32]. The pre-treatment consisted in applying a series of pulses: oxidation at a potential $E_{ox} = E_{app.}^{0\prime} + 320$ mV, reduction at $E_{red} = E_{app.}^{0\prime} - 360$ mV, and a final oxidation to E_{ox}; where $E_{app.}^{0\prime}$ is the apparent formal potential of the Pu(IV)/Pu(III) redox couple in a HNO_3 0.9 mol L^{-1} medium (during the standard CPC analyses of Pu, $E_{app.}^{0\prime} =$

675 mV / SCE). Each pulse was applied until a chosen current threshold (10 µA for the oxidative phases and - 10 µA for the reductive phases) was reached.

It is important to note that as $E^{0\prime}_{app.}$ only takes into account the effect of ionic strength and the interaction between the nitrate anions and the Pu cations in a HNO_3 0.9 mol L^{-1} medium, it does not correspond to the formal potential of the Pu(IV)/Pu(III) redox couple in the studied media (where sulfates are present as a consequence of the H_2SO_4 fuming procedure). The value of $E^{0\prime}_{app.}$ used during these experiments (675 mV / SCE) was chosen based on the reported literature values for the formal potential of the Pu(IV)/Pu(III) redox couple in 1 mol L^{-1} HNO_3 [18,24,33]. The true formal potential of the Pu(IV)/Pu(III) redox couple in the studied media (henceforth denoted as $E^{0\prime}_{Pu(IV)/Pu(III)}$ in the present paper) was determined experimentally through the means of a coulogram (described later in the text) following CPC analysis.

3) Blank measurement

In the same medium used for the pre-treatment procedure, a blank measurement was performed. During the blank measurement, a reductive potential E_1 (defined in relation to $E^{0\prime}_{app.}$ as shown in equation (2)) was applied to the working electrode, followed by an oxidative potential E_2(defined as shown in equation (3)). During the latter step, the duration of oxidation (t_1), residual current (i_{r1}), and raw quantity of electrical charge used (Q_1) were recorded. Each electrochemical phase was performed until a stable current of 1 µA or a drift inferior to 1 µA / 100 s was observed. The potentials applied during the blank measurement phases were the same as those used subsequently during the analysis of Pu.

$$E_1 = E^{0\prime}_{app.} - 230 \text{ mV} \qquad (2)$$

$$E_2 = E^{0\prime}_{app.} + 230 \text{ mV} \qquad (3)$$

It is worth noting that the size of Q_1 is particularly important, as it will determine the detection limit of the analytical technique. During standard CPC analyses of Pu it is recommended that Q_1 not exceed 5 mC, corresponding to a minimum possible mass of 12 µg of Pu in an analysed solution [31].

4) Coulometric analysis of Pu

The electrolyte used for the pre-treatment and blank measurements was transferred to a coulometric cell containing the dried sample to be analysed. The dried sample was dissolved in the solution through mild agitation. After this, the analysis procedure consisted in applying a reducing potential E_1 to convert the Pu(IV) in the test sample to Pu(III), followed by an oxidising potential E_2 which converted the generated Pu(III) into Pu(IV). Both phases were applied until a stable current of 1 µA or a drift inferior to 1 µA/100 s was observed. The shift of ± 230 mV from $E^{0\prime}_{app.}$ (seen in equations (2) and (3)) was chosen such that, if $E^{0\prime}_{app.} = E^{0\prime}_{Pu(IV)/Pu(III)}$, the degree of completion of the electrochemical reactions would correspond

to 99.99%. During the oxidation step, the duration of oxidation (t_2), residual current (i_{r2}), and raw quantity of electrical charge used (Q_2) were measured.

In order to calculate the net quantities of electrical charge used for the oxidation of the blank (Q_b) and the analysed sample (Q_s), the raw quantities of electrical charge (Q_1 and Q_2) were corrected to take into account the residual current in each phase, as shown in equations (4) and (5):

$$Q_b = Q_1 - i_{r1}t_1 \qquad (4)$$

$$Q_s = Q_2 - i_{r2}t_2 \qquad (5)$$

Q_s and Q_b were then incorporated into Faraday's law as shown in equation (6) in order to calculate the mass of Pu in the studied sample from the net charge.

$$m_{Pu} = \frac{(Q_s - Q_b)\, M_{Pu}}{n\, F\, f} \qquad (6)$$

The introduction of the f factor in equation (6) is crucial. This corrective factor, named the "electrolysed fraction", is derived from Nernst's law and takes into account the fraction of Pu(IV) not reduced during the first step of the Pu analysis, as well as the fraction of Pu(III) not oxidised during the second step of the procedure [34]. Mathematically, the f factor is expressed as shown in equation (7) where E_1 and E_2 are the potentials applied during the reduction and oxidation phases of the analysis, $E^{0\prime}_{Pu(IV)/Pu(III)}$ is the experimental formal potential of the Pu(IV)/Pu(III) redox couple in the studied medium, n is the number of electrons exchanged (1 for the Pu(IV)/Pu(III) redox couple), F is Faraday's constant, R is the molar gas constant, and T is the temperature of the bulk (in K).

$$f = \frac{\exp\left(\frac{n\,F\,\left(E_2 - E^{0\prime}_{Pu(IV)/Pu(III)}\right)}{RT}\right)}{1 + \exp\left(\frac{n\,F\,\left(E_2 - E^{0\prime}_{Pu(IV)/Pu(III)}\right)}{RT}\right)} - \frac{\exp\left(\frac{n\,F\,\left(E_1 - E^{0\prime}_{Pu(IV)/Pu(III)}\right)}{RT}\right)}{1 + \exp\left(\frac{n\,F\,\left(E_1 - E^{0\prime}_{Pu(IV)/Pu(III)}\right)}{RT}\right)} \qquad (7)$$

It can be seen from equation (7) that the fraction of non-electrolysed Pu during each analysis stage is dependent on the difference between the applied potentials E_1 and E_2 and the formal potential of the Pu(IV)/Pu(III) redox couple in the studied medium. As such, it becomes evident that the formal potential of the Pu(IV)/Pu(III) redox couple needs to be precisely known for each studied medium in order to achieve a high analytical accuracy.

Coulograms for the measure of $E^{0\prime}_{Pu(IV)/Pu(III)}$

In order to calculate the f factor, the formal potential of the Pu(IV)/Pu(III) redox couple was determined by recording coulograms of the studied solutions in the same conditions as those used

for the coulometric analyses. In a coulogram, the quantity of electric charge (Q) required to reach equilibrium (defined as a very low current condition, I ≤ 50 µA) starting from a completely reduced solution is plotted as a function of the potential applied to the working electrode (E). The formal potential of the studied couple can be taken from the inflexion point of the curve plotted in the coulogram, in the present study this corresponds to the potential at which Pu(IV) and Pu(III) are present in the solution in equal proportions. This inflexion point can be determined by plotting $\ln(Q/(Q_{max}-Q))$ (where Q_{max} is the maximum value of Q) as a function of E, the x-intercept of the plotted line corresponds to the formal redox potential of the studied couple. An example of the graphs used for the determination of a given sample's formal potential through a coulogram can be seen in the supporting information of this paper (Appendix A, section A.1, figures A.1 and A.2).

Cyclic voltammetry experiments

The evolution of the formal potential of the Pu(IV)/Pu(III) redox couple was studied through cyclic voltammetry in the same conditions as those used for the coulometric analyses. In the cyclic voltammetry experiments, the current response of the WE was recorded between + 50 mV / SCE and + 1100 mV / SCE at a scan rate of 10 mV s^{-1}. Each scan was performed for two cycles with the second cycle being retained for the analysis of the studied samples.

Sulfate analysis

The sulfate content of the analysed solutions was determined through ion chromatography (ThermoElectron (DIONEX) ICS 5000). The ion chromatograph was equipped with an autosampler, a potassium hydroxide (KOH) eluent generator, an electrolytic suppressor, and a conductivity detector. Ion separation was performed through an IonPac AS10 capillary column (0.4 X 250 mm) preceded by an IonPac AG10 guard column (0.4 X 50 mm), both columns possess alkanol quaternary ammonium functionalisation.

In order to perform the sulfate analyses, the solutions previously used for the electrochemical analyses were filtered through a 0.2 µm Millipore filter and diluted in sodium hydroxide (NaOH, 80 mmol L^{-1}) such that the estimated sulfate concentration of each analyte was within the equipment's operating range (0 – 5 mg L^{-1}) .

Chemical speciation calculations

The speciation of Pu + U nitric acid solutions was simulated through the PhreeqC geochemical calculation software (version 3.5.0.14000) coupled with the PhreeqCI (Version 3.5.0.14000) interface and the NEA TDB database for PhreeqC (version 1.0). The NEA database was amended to include the ionic interaction coefficients ($\varepsilon\ (i,k)$, determined as described in this paper's supporting information (Appendix A, section A.2)) for the various species present in solution.

The distribution of different species in solution is determined by PhreeqC from the thermodynamic equilibrium constants, K, of the complexation reactions between the various anions and cations present in the solution. The general equation for the complexation between a species M and a ligand L is expressed as shown in equation (8) (where p and q are the stoichiometric quantities of the species).

$$pM + qL \leftrightarrows M_pL_q \qquad (8)$$

The equilibrium constant, K_m, for the complexation reaction shown in equation (8) is expressed in terms of the different species' thermodynamic activities, a, molal concentrations, and activity coefficients, γ, as shown in equation (9).

$$K_m = \frac{a_{ML}}{{a_M}^p \ {a_L}^q} = \frac{[M_p L_q]}{[M]^p \ [L]^q} \frac{\gamma_{ML}}{{\gamma_M}^p \ {\gamma_L}^q} \qquad (9)$$

The activity coefficients for the species in solution were determined in terms of the molal ionic strength, I_m, of the solution, expressed as shown in equation (10) where m_i and Z_i are the molal concentration and charge of species i, respectively. In the current experiment, the I_m of the studied Pu + U solutions (U:Pu = 95.6) was calculated to be 0.970 molal.

$$I_m = \frac{1}{2} \sum_i m_i \, {Z_i}^2 \qquad (10)$$

I_m is related to the activity coefficients of the studied species in solution by the Brønsted-Guggenhein-Scatchard model (also known as the Specific Ion Interaction Theory, SIT) wherein the activity coefficient, γ_i, of an ionic species, i, can be expressed as shown in equation (11):

$$\log(\gamma_i) = -\frac{Z_i^2 \, A^2 \sqrt{I_m}}{1 + 1.5\sqrt{I_m}} + \sum_k \varepsilon \, (i,k) \, m_k \qquad (11)$$

Where A is the Debye-Hückel limiting slope (a function of temperature and pressure, at the experimental conditions of 1 bar and 21 °C, A = 0.506 $kg^{1/2}$ $mol^{-1/2}$ [35]) , m_k is the molality of species k, and $\varepsilon \, (i,k)$ is a SIT coefficient (also known as an ion interaction parameter) which describes the short-range electronic interaction between aqueous species i and k. The thermodynamic equilibrium constants (in molal units) as well as the SIT coefficients supplied in the NEA TDB and used by PhreeqC are values at 298.15 K and I_m = 0. These values were extrapolated by PhreeqC to (and from) media with non-zero ionic strengths as described by Grenthe and co-workers [35,36].

In the present experiments, U (VI) and Pu (IV) sulfate crystals were dissolved in aqueous HNO_3 for CPC analysis. It has been previously shown that in aqueous acidic solutions containing HNO_3 (at concentrations between 0.1 and 4 mol L^{-1}), Pu^{4+} will only complex as the mono- or di- nitrate form [37] whilst UO_2^{2+} will be present as the mono-, di-, and tri- nitrate complexes [38] (in addition to the free cation species). In aqueous acidic solutions containing H_2SO_4, Pu^{3+} will tend to form the mono-sulfate complex, [39] Pu^{4+} will tend to form the mono- and di- sulfate complexes [39,40], and UO_2^{2+} will form mono-, di-, and tri- sulfate complexes [38,41,42]. It is also known that both Pu^{3+} and Pu^{4+} can undergo hydrolysis in acidic conditions, forming $PuOH^{2+}$ and $PuOH^{3+}$ [37,43]. Due to the lack of consensus and the difficulty of experimental measurement regarding the values of the thermodynamic properties of $UO_2(NO_3)_3^-$ and the Pu(III)-nitrate complexes, their formations are not included in the TDB database and were thus not considered for the simulations performed during this experiment.

As such, for the purpose of determining SIT coefficients, it was assumed that the studied solutions contained the aqueous charged ions $Pu^{4+}{}_{(aq)}$, $PuNO_3^{3+}{}_{(aq)}$, $PuSO_4^{2+}{}_{(aq)}$, $PuOH^{3+}{}_{(aq)}$, $Pu^{3+}{}_{(aq))}$, $PuSO_4^{+}{}_{(aq)}$, $PuOH^{2+}{}_{(aq)}$, $UO_2^{2+}{}_{(aq)}$, $UO_2NO_3^{+}{}_{(aq)}$, $UO_2(SO_4)_2^{2-}{}_{(aq)}$, $UO_2(SO_4)_3^{4-}{}_{(aq)}$, $HSO_4^-{}_{(aq)}$, $SO_4^{2-}{}_{(aq)}$, and $NO_3^-{}_{(aq)}$. The equilibrium constants used by PhreeqC during this experiment's speciation studies for the formation of the Pu and uranyl complexes as well the protonation of the sulfate anion, are supplied with the NEA TDB and are shown in table 1. Table 1 also shows the equilibrium constants as calculated by PhreeqC at the experimental conditions of the studied Pu + U solutions (U:Pu = 95.6). It can be seen

from table 1 that, in accordance with expectations, the equilibrium constants for the studied reactions are lower in non-zero ionic media. This is due to the electrostatic interactions between the various ions present in the medium, which affect the activity coefficients of the ions involved in the studied complexation reactions.

Table 1: *Thermodynamic equilibrium constants supplied in the NEA TDB and used by PhreeqC for the speciation of the main complexes formed in the studied solutions.*

Reaction	$\log(K_m^0)$ [a]	$\log(K_m^*)$ [b]
$SO_4^{2-} + H^+ \rightleftharpoons HSO_4^-$	1.98	1.48
$UO_2^{2+} + SO_4^{2-} \rightleftharpoons UO_2SO_4$	3.15	1.92
$UO_2^{2+} + 2\ SO_4^{2-} \rightleftharpoons UO_2(SO_4)_2^{2-}$	4.14	3.15
$UO_2^{2+} + NO_3^- \rightleftharpoons UO_2NO_3^+$	0.30	-0.36
$Pu^{3+} + SO_4^{2-} \rightleftharpoons PuSO_4^+$	3.91	1.69
$Pu^{3+} + H_2O \rightleftharpoons PuOH^{2+} + H^+$	-6.90	-7.70
$Pu^{4+} + SO_4^{2-} \rightleftharpoons PuSO_4^{2+}$	6.89	3.90
$Pu^{4+} + 2\ SO_4^{2-} \rightleftharpoons Pu(SO_4)_2$	11.14	7.01
$Pu^{4+} + NO_3^- \rightleftharpoons PuNO_3^{3+}$	1.95	0.53
$Pu^{4+} + H_2O \rightleftharpoons PuOH^{3+} + H^+$	0.60	-0.61

[a] *Equilibrium constants as supplied in the NEA TDB, valid at I_m = 0 and T = 298.15 K.*

[b] *Equilibrium constants at the experimental conditions of the studied Pu + U solutions (U:Pu = 95.6, I_m = 0.970, T = 294.15 K) as calculated by PhreeqC.*

As $UO_2(SO_4)_3^{4-}$ has been shown to be present only in minute quantities in experimental conditions similar to those of the present experiment [38,41,42,44], its $\varepsilon\ (i,k)$ values were considered negligible and not taken into account for the speciation simulations. The remaining SIT coefficients used during this study are reported in table 2. Generally, SIT coefficients for a large number of ion pairs have been determined experimentally and can be found in literature [43,45]. For the cases where SIT coefficients are not obtainable from literature, it is often recommended that the $\varepsilon\ (i,k)$ values of analogous systems or mathematical extrapolation methods be used to determine approximate values [35,43]. In the present work, unknown $\varepsilon\ (i,k)$ values were estimated by using the methods presented by Vercouter *et al.* [46], Tkac *et al.* [47], and Ciavatta [36,48], as described In this paper's supporting information (Appendix A, section A.2).

Table 2: *$\varepsilon\ (i,k)$ coefficients used for the speciation studies performed during the present experiment (I = 0 and T = 298.15 K). For clarity, values originating directly from literature sources have been italicised.*

		k			
		SO_4^{2-}	HSO_4^-	NO_3^-	$UO_2(SO_4)_2^{2-}$
i	H^+	*0.24* [a]	*0.10* [a]	*0.07* [b]	*- 0.08* [a]
	Pu^{3+}	0.69 [c]	0.29 [d]	0.22 [e]	- 0.37 [f]
	Pu^{4+}	1.32 [c]	0.55 [d]	*0.31* [g]	- 0.56 [f]
	UO_2^{2+}	*- 0.20* [a]	*0.35* [a]	*0.24* [b]	*- 0.13* [a]
	$PuSO_4^+$	0.47 [h]	0.27 [h]	0.23 [h]	- 0.07 [h]
	$PuSO_4^{2+}$	0.78 [h]	0.40 [h]	0.28 [i]	- 0.16 [h]
	$UO_2NO_3^+$	-0.07 [h]	0.21 [h]	0.16 [h]	- 0.03 [h]
	$PuNO_3^{3+}$	0.70 [h]	0.31 [h]	0.19 [h]	- 0.25 [h]
	$PuOH^{2+}$	0.36 [h]	0.16 [h]	0.13 [h]	-
	$PuOH^{3+}$	0.68 [h]	0.29 [h]	0.23 [e]	-

[a] Taken from Alcorn et al. [41] *[b] Supplied in the NEA TDB PhreeqC database (version 1.0, November 2018). [c] Estimated using the linear regression technique established by Vercouter et al.* [46]. *[d] Estimated from the linear correlation reported by Vercouter et al.*[46]. *[e] Estimated from the linear regression technique previously used by Paulenova* [37]*, Tkac et al.* [47]*, and Neck et al.* [49]. *[f] Estimated from the correlations established by Alcorn et al.* [41]. *[g] Taken from Tkac et al.* [47]. *[h] Estimated using the method reported by Ciavatta.* [48]. *[i] Used the value for* $\varepsilon\ (ThSO_4{}^{2+}, NO_3{}^{-})$ *estimated from the technique established by Neck et al.*[49]

In order to replicate laboratory conditions, the PhreeqC simulations were performed on 30 mL solutions at 21 °C containing HNO_3, SO_4^{2-}, UO_2^{2+}, Pu^{4+}, and Pu^{3+} in concentrations equal to those encountered during the laboratory experiments. The density of the simulated solutions was determined from the concentrations of U, Pu, and HNO_3 in the solutions at 21 °C by using the equation previously developed by Kumar and Koganti [50]. From this, the density of the solutions varied between 1.0217 g mL^{-1} (for a 0.9 mol L^{-1} HNO_3 solution where U:Pu = 0) and 1.0375 g mL^{-1} (for a 0.9 mol L^{-1} HNO_3 solution where U:Pu = 120). The pH of the solutions varied between 0.181 and 0.204.

Results and analysis

1 – Sulfate analysis results

The individual results of the sulfate analyses for a series of mixed Pu + U samples (YD 50, YD51, YD54, YD55, and YD57) originating from a standard initial solution with a U:Pu ratio of 95.6 (EQRAIN (U+Pu) n°02, vials # S061, S074, and S089) are shown in the supporting information of this paper (Appendix A, section A.3, figure A.5). From these results it was observed that the average total concentration of

sulfates, $C_{sulfate}$, in the mixed Pu + U samples (50 ± 13 mmol L^{-1}) (k=2) is consistent with the value calculated from the stoichiometry of the $Pu(SO_4)_2$ and UO_2SO_4 crystals (48.2 ± 1.5 mmol L^{-1}) (k=2); created during the fuming phase of the sample preparation procedure (such that $n_{SO_4} = 2\,n_{Pu} + 1\,n_U$). This confirms that the actinide sulfate crystals are the sole source of sulfate anions in the analysed CPC solutions and that excess sulfate from the added H_2SO_4 has been eliminated in the form of sulphur trioxide (SO_3) gas during the fuming step.

2 – Cyclic voltammetry and coulogram results

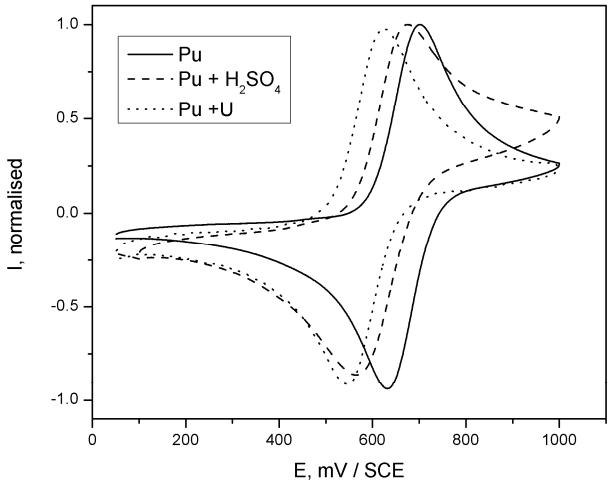

Figure 2: *Cyclic voltammograms showing the electrochemical response of the* Pu(IV)/Pu(III) *redox couple in representative solutions of Pu nitrate (solid line, sample YD 60), Pu + H_2SO_4 (dashed line, sample YD 63), and Pu + U (dotted line, sample YD 51) in HNO_3 (0.9 mol L^{-1}). The scans were performed at a rate of 10 mV s^{-1} with an Au mesh working electrode. The curves have been normalised with respect to the maximum peak current response for each sample.*

The cyclic voltammograms and coulograms for solutions containing pure Pu (sample YD 60), Pu + U (U:Pu = 95.6, sample YD 51), and Pu + H_2SO_4 (sample YD 63) are presented in figures 1 and 2, respectively. The three specific solutions presented in these figures (YD 60, YD 51, and YD 63) were chosen as representative samples for the whole series of repetitions performed on each solution type. The data presented in figures 2 and 3 has been normalised for clarity as the different samples studied contained different quantities of Pu, which affect the magnitude of the current response.

The redox peak distances in figure 2 were calculated to be 69, 95, and 76 mV for the Pu, Pu + H_2SO_4, and Pu + U solutions. The relative proximity of the peak-to-peak distances demonstrated that the addition of H_2SO_4 and U did not significantly affect the electron transfer kinetics between the systems, allowing the Pu(IV)/Pu(III) redox couple to remain electrochemically reversible. It has been previously established [51] that the formal potential of a quasi-reversible redox couple can be estimated from a voltammogram by taking the midpoint between the couple's redox peaks. As such, from the data presented in figure 2 an $E^{0'}_{Pu(IV)/Pu(III)}$ of 667, 624, and 588 mV / SCE was estimated

for the studied Pu (sample YD 60), Pu + H_2SO_4 (sample YD 63), and Pu + U (sample YD 51) solutions, respectively.

A better estimate of a redox couple's formal potential can be obtained by studying the couple's coulogram. As such, this technique was used exclusively throughout this study for the CPC and $E^{0\prime}_{Pu(IV)/Pu(III)}$ analyses. From the coulograms shown in figure 3 it was thus possible to calculate $E^{0\prime}_{Pu(IV)/Pu(III)}$ in the studied solutions: $E^{0'}_{Pu(III)/Pu(IV)} = 671$ mV / SCE for pure Pu (sample YD 60); 636 mV / SCE for Pu + H_2SO_4 (sample YD 63); and 595 mV / SCE for Pu + U (sample YD 51).

It can be seen from both figures 2 and 3 that $E^{0\prime}_{Pu(IV)/Pu(III)}$ in the mixed solutions is cathodically shifted with respect to that observed in the pure solutions. The occurrence of this shift in both the Pu + H_2SO_4 and Pu + U solutions, as well as the comparable peak shapes of the Pu and Pu + U solutions in figure 2 indicate that – in accordance with literature expectations [11,17] and the redox peak potentials of the UO_2^{2+}/U^{4+}couple [52] – the presence of sulfate anions rather than the uranyl cations is the most probable cause of the observed shift.

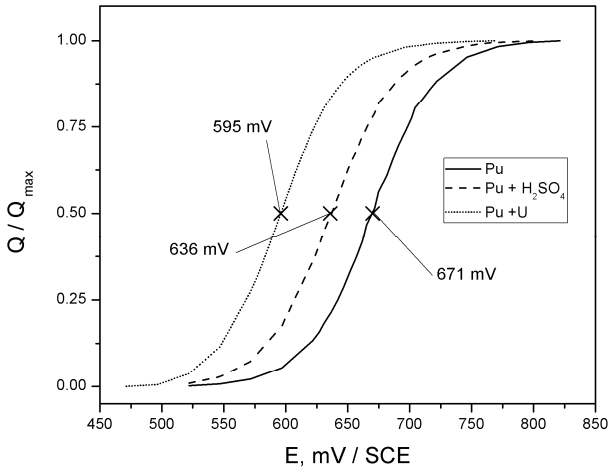

Figure 3: *Coulograms of representative Pu (solid line, sample YD 60), Pu + H_2SO_4 (dashed line, sample YD 63), and Pu + U (dotted line, sample YD 51) solutions in HNO_3 (0.9 mol L^{-1}). The inflexion point of each curve (corresponding to the solution's $E^{0\prime}_{Pu(IV)/Pu(III)}$) has been marked.*

As such, the observed shift in $E^{0\prime}_{Pu(IV)/Pu(III)}$ can be attributed to an interaction between the sulfate ligands and Pu cations in the studied solutions. This can be seen more clearly from the collated data of all of the experiments performed for each solution series presented in table 3 where increasing concentrations of total SO_4^{2-} in solution are accompanied by a decrease in $E^{0\prime}_{Pu(IV)/Pu(III)}$. By using computational simulations, it was possible to clarify the origin of this shift and the precise role played by sulfate anions in the studied solutions.

Table 3: *Evolution of $E^{0\prime}_{Pu(IV)/Pu(III)}$* in relation to the total concentration of sulfates in solution for the three types of solution studied during the present experiment.

Solution	SO_4 : Pu	$C_{sulfate}$ (mmol L^{-1})	$E^{0\prime}_{Pu(IV)/Pu(III)}$ (mV / SCE)
Pure Pu [a]	2.0 ± 0.1	1.50 ± 0.05	671 ± 5
Pu + H_2SO_4 [a, b]	25 ± 1	22.5 ± 0.7	636 ± 5
Pu + U [a, c]	110 ± 26	50 ± 13	599 ± 16

[a] The errors for the Pu and Pu + H_2SO_4 samples are taken at k=2 whilst the error on the Pu + U samples corresponds to two times the standard deviation of the measurements (2s). [b] Results corresponding to the mean of 3 measurements. [c] Results corresponding to the mean of 11 measurements.

2 – *Speciation Results*

The speciation of the main (concentrations > 1 µmol L^{-1}) species present in the studied Pu + U solutions in aqueous HNO_3, as simulated through PhreeqC, are shown in relation to the U:Pu molar ratio and the total sulfate concentration in the system ($C_{sulfate}$) in figure 4 *(*middle and lower graphs for the speciation of U and Pu, respectively). The numerical values for the simulated distribution of the main species in the three different types of solution studied during this experiment can be found in the supporting information of this paper (Appendix A, section A.4, table A.3).

In order to replicate the experimental conditions wherein the SO_4^{2-} anions are brought into solution by the $Pu(SO_4)_2$ and UO_2SO_4 crystals generated from the sample fuming procedure, the sulfate anions in the simulations were introduced in conjunction with UO_2^{2+} cations in appropriate stoichiometric quantities. As such, the increase in total sulfate concentration, $C_{sulfate}$, in figure 4 is accompanied by equimolar increases in $C_{UO_2^{2+}}$ to replicate the increasing quantity of UO_2SO_4 crystals in solutions with increasing U:Pu ratios. This can be seen in the top graph of figure 4 where the concentration of free sulfate ligands (HSO_4^- and SO_4^{2-}) directly follow the total concentration of U in the systems.

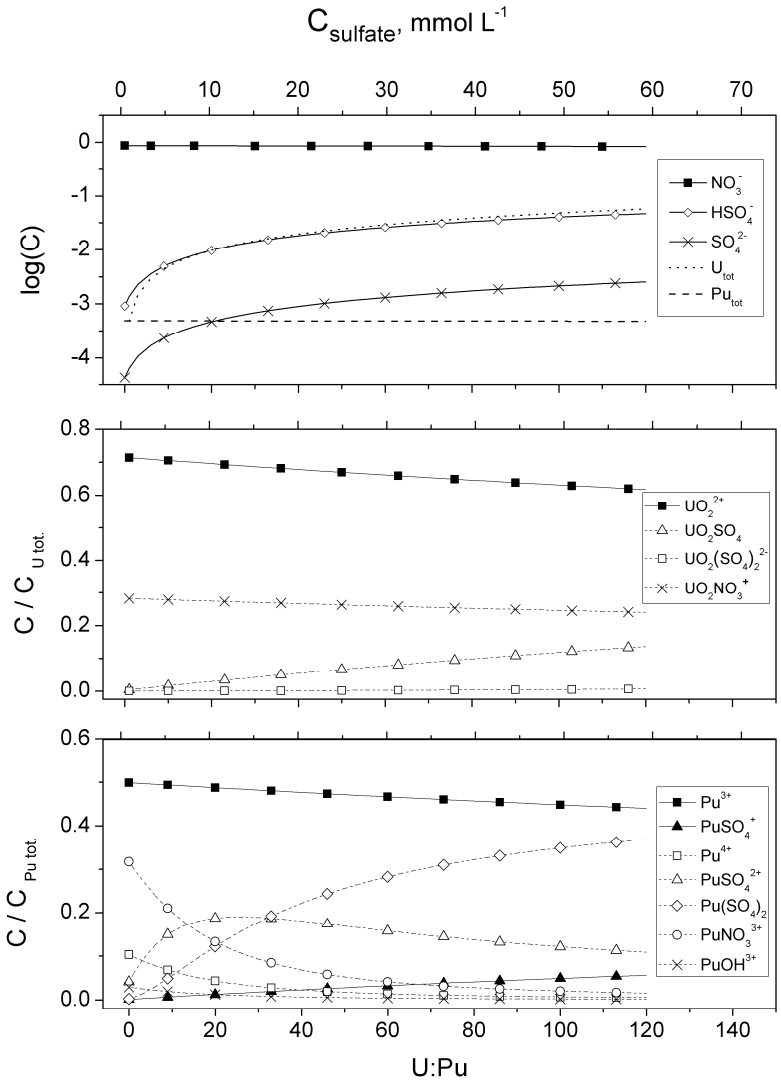

Figure 4: *Results of the PhreeqC simulations showing the evolution of different species as UO_2SO_4 crystals ([UO_2^{2+}] = 0 - 57.6 mmol L^{-1}) are dissolved in aqueous HNO_3 (0.9 mol L^{-1}) solutions containing Pu (0.490 mmol L^{-1}, composed by equimolar quantities of Pu(III) and Pu(IV)) in relation to the solutions' U:Pu ratio (or total sulfate concentration, $C_{sulfate}$). Upper: evolution of free ligand concentrations in relation to the concentration of actinides in solution. Middle: speciation distribution of significant uranyl species. Bottom: speciation of significant Pu(IV) and Pu(III) species.*

From the speciation of U in solution (figure 4, middle graph), it can also be observed that once dissolved in HNO_3, the UO_2SO_4 crystals dissociate readily, leading to UO_2^{2+} being the primary form of U in solution, comprising 71% of the total U species when C_{SO_4} = 1.47 mmol L^{-1} (U:Pu = 1) and 63% of the total U species when $C_{sulfate}$ = 47.2 mmol L^{-1} (U:Pu = 95.6). This predominance of the UO_2^{2+} cation is consistent with the relatively small formation constants for the UO_2SO_4, $UO_2(SO_4)_2^{2-}$, and $UO_2NO_3^+$ complexes (log(K_m^*) = 1.92, 3.15, and -0.36, respectively), as seen in table 1. Therefore, each addition of UO_2SO_4 crystals to the studied solutions will lead to a significant increase in quantity of free HSO_4^- and SO_4^{2-} ions, which remain available for complexation with other species present in solution (such as the Pu^{3+} and Pu^{4+} cations).

The evolution of the concentration of free sulfate and nitrate (NO_3^-) anions as well as the total concentrations of U and Pu are shown in the top graph of figure 4 as a function of both the U:Pu ratio total sulfate concentration in the solutions. It can be seen that, in accordance with the dissociation constants of H_2SO_4 (- 8.6 ≤ pKa_1 ≤ -4.5 and [53], and pKa_2 = 1.99 [54]), at the studied pH levels (0.181 – 0.204) the mono-protonated HSO_4^- will be the dominant form of sulfate species in solution. Furthermore, the amount of free sulfate anions in solution increases with the amount of U added to the systems. This increasing availability of free sulfate anions relative to total Pu in solution can be expected to play a significant role in the actinide's speciation in the studied systems.

The effect of free sulfate anions on the speciation of Pu ions in solutions containing equimolar quantities of Pu(IV) and Pu(III) can be seen in the lower graph of figure 4. In this graph, where three ($PuSO_4^+$, $PuSO_4^{2+}$, $Pu(SO_4)_2$) of the five main complexes formed by the Pu cations are sulfate complexes (respectively composing 4.8%, 12%, and 35% of the total Pu in solution at U:Pu = 95.6). It is important to note that, as a consequence of the large differences between the complexation constants for the sulfate species in solution (as seen in table 1), Pu(IV) is more likely to be complexed with sulfate anions than Pu(III). Indeed, the complexation constant for the formation of $PuSO_4^+$ ($\log(K_m^*)$ = 1.69) is much smaller than those for the formation of $PuSO_4^{2+}$ ($\log(K_m^*)$ = 3.90) and $Pu(SO_4)_2$ ($\log(K_m^*)$ = 7.01), resulting in the amount of free Pu^{3+} in solution being much greater than that of Pu^{4+} . This is seen in figure 4 (bottom graph) where at low $C_{sulfate}$ (1.47 mmol L^{-1}, corresponding to U:Pu = 1), Pu(III) is present primarily as the Pu^{3+} cation (49.8% of the total Pu in solution) with only a minor amount of Pu(III) present as a complex ($PuSO_4^+$, 0.18% of the total Pu in solution). At the same sulfate concentration, Pu(IV) is present as three different species: the $PuNO_3^{3+}$ nitrate complex (30% of the total Pu), the $PuSO_4^{2+}$ sulfate complex (5.9% of the total Pu), and the uncomplexed Pu^{4+} cation (9.8% of the total Pu). Although the complexation constant for the formation of $Pu(SO_4)_2$ is significantly larger than that of the other Pu-sulfate complexes, its presence at low concentrations of SO_4^{2-} in solution remains relatively small (0.53% of the total Pu) due to the low availability of the complexing anion.

As $C_{sulfate}$ is increased (to $C_{sulfate}$ = 47.2 mmol L^{-1}, corresponding to U:Pu = 95.6) , a change occurs in the distribution of the Pu species due to the increased presence of complexing anions in solution. In the case of the Pu(III) valence, this change remains limited: although the proportion of the $PuSO_4^+$ complex relative to the free Pu^{3+} cation increases (accounting for 4.75% of the total Pu), the free cation remains the dominant species in solution (45% of the total Pu). However, in the case of the Pu(IV) valence, as $C_{sulfate}$ increases to 47.2 mmol L^{-1} , the relative concentrations of $PuNO_3^{3+}$ and Pu^{4+} decrease significantly, (to 2.1%, and 0.71% of the total Pu, respectively), whilst the concentrations of $PuSO_4^{2+}$ and $Pu(SO_4)_2$ increase (to 12% and 35% of the total Pu, respectively) with the latter complex becoming the dominant species. The dominance of the $Pu(SO_4)_2$ complex occurs due to the large availability of free sulfate anions in solutions, as seen in the top graph in figure 4.

This uneven complexation of sulfate ions between Pu^{3+} and Pu^{4+} cations, exacerbated by the increasing sulfate concentrations, will induce a shift in the $E^{0\prime}_{Pu(IV)/Pu(III)}$ of the solutions. Indeed, the electrochemical potential , E, of a given medium can be expressed through Nernst's equation as shown in equation (12) where $E^{\circ}{}_{Pu(IV)/Pu(III)}$ is the standard potential of the redox couple at temperature T; R is the ideal gas constant; F is Faraday's constant; T is the temperature of the medium (in K); $a_{Pu^{4+}}$ and $a_{Pu^{3+}}$ are the activities of the free Pu^{4+} and Pu^{3+} cations, respectively [26].

$$E = E^{\circ}{}_{Pu(IV)/Pu(III)} + \frac{R\,T}{F}\ln\left(\frac{a_{Pu^{4+}}}{a_{Pu^{3+}}}\right) \qquad (12)$$

The activity of a species i is the product of its concentration and activity coefficient. As such, it is possible to express equation (12) as equation (13) where $[Pu^{4+}]$ and $[Pu^{3+}]$ are the concentrations of free Pu^{4+} and free Pu^{3+}, respectively; $\gamma_{Pu^{4+}}$ is the activity coefficient of Pu^{4+}; and $\gamma_{Pu^{3+}}$ is the activity coefficient for Pu^{3+}.

$$E = E°_{Pu(IV)/Pu(III)} + \frac{R\,T}{F}\ln\left(\frac{[Pu^{4+}]\gamma_{Pu^{4+}}}{[Pu^{3+}]\,\gamma_{Pu^{3+}}}\right) \qquad (13)$$

Equation (13) can be simplified by introducing $E^{\circ}_{app.\ Pu(IV)/Pu(III)}$, a term for the apparent potential of the redox couple at temperature T (taking into account the effect of ionic strength), as shown in equation (14).

$$E = E^{\circ}_{app.\ Pu(IV)/Pu(III)} + \frac{R\,T}{F}\ln\left(\frac{[Pu^{4+}]}{[Pu^{3+}]}\right) \qquad (14)$$

However, equation (14) does not take into account the cation complexation occurring in the current experiment. As the concentration of sulfate ions in the studied solutions increases, the sulfate complexation of the Pu^{4+} and Pu^{3+} cations becomes predominant, diminishing the molality of free cations. The extent of this complexation can be quantified in terms of the total concentration of each oxidative state of Pu by the complexation coefficient α as shown in equation (15) for both Pu cations (where $C_{Pu(III)}$ and $C_{Pu(IV)}$ are the total concentrations of the Pu(III) and Pu(IV) valences, respectively).

$$\alpha_{Pu(III)} = \frac{C_{Pu(III)}}{[Pu^{3+}]} \qquad \alpha_{Pu(IV)} = \frac{C_{Pu(IV)}}{[Pu^{4+}]} \qquad (15)$$

Equation (19) can thereby incorporate the complexation of the Pu cations as shown in equation (16).

$$E = E^{\circ}_{app\ Pu(IV)/Pu(III)} + \frac{R\,T}{F}\ln\left(\frac{\alpha_{Pu(III)}}{\alpha_{Pu(IV)}}\right) + \frac{R\,T}{F}\ln\left(\frac{C_{Pu(IV)}}{C_{Pu(III)}}\right) \qquad (16)$$

In the studied conditions, where the two Pu valences are present in equimolar quantities, the potential of the solution becomes the formal potential of the Pu(IV)/Pu(III) redox couple ($E^{0\prime}_{Pu(IV)/Pu(III)}$), allowing this special case to be expressed as equation (17).

$$E^{\circ\prime}{}_{Pu(IV)/Pu(III)} = E^{\circ}_{app.\ Pu(IV)/Pu(III)} + \frac{R\,T}{F}\ln\left(\frac{\alpha_{Pu(III)}}{\alpha_{Pu(IV)}}\right) \qquad (17)$$

It becomes apparent that the preferential complexation of Pu(IV) by the sulfates and nitrates relative to Pu(III), will have an important effect on the $E^{0\prime}_{Pu(III)/Pu(IV)}$ of studied solutions. Indeed, as the concentration of sulfates in the system increases, the disproportional increase of $\alpha_{Pu(IV)}$ relative to $\alpha_{Pu(III)}$ will result in a reduction in the $\ln\left(\frac{\alpha_{Pu(III)}}{\alpha_{Pu(IV)}}\right)$ term which, as seen in equation (17), will induce a cathodic shift of the $E^{0\prime}_{Pu(III)/Pu(IV)}$ of studied solutions. This effect can be visualised more clearly in figure A.6 of the supporting information of this paper (Appendix A, section A.5) where the evolution of $\ln(\alpha_{Pu(III)})$, $\ln(\alpha_{Pu(IV)})$, and $\ln\left(\frac{\alpha_{Pu(III)}}{\alpha_{Pu(IV)}}\right)$ for the simulated solutions are shown in relation to the solutions' total concentration of sulfates, $C_{sulfate}$(and the U:Pu ratio).

The evolution of $E^{o\prime}{}_{Pu(IV)/Pu(III)}$ for solutions containing equimolar amounts of Pu(III) and Pu(IV), calculated from the speciation simulations in relation to the total sulfates in solution, $C_{sulfate}$, and the U:Pu ratio of the solutions, is presented in figure 5 in conjunction with the present study's experimental values as well as the values previously reported by *Ruas et al.* [11]. The simulated values can be seen to lie within the confidence intervals of the experimental data, demonstrating a good correlation between the theoretical and simulated data. This confirms that the cathodic shifts in $E^{0\prime}_{Pu(IV)/Pu(III)}$ observed experimentally between Pu and Pu + U solutions (as seen in table 3), can be attributed to the complexation of Pu by SO_4^{2-} anions; which originate mostly from the UO_2SO_4 crystals created during the sample preparation procedure used for the coulometric analysis of Pu. Furthermore, the strong correlation between the two sets of data demonstrates that PhreeqC speciation simulations can be used to estimate the $E^{0\prime}_{Pu(IV)/Pu(III)}$ of studied Pu + U solutions from the concentration of sulfates (or the U:Pu ratio) in the solutions. Whilst it is important to note that such a method cannot supplant the use of a coulogram for the determination of a studied solution's $E^{0\prime}_{Pu(IV)/Pu(III)}$, it can provide a good estimate from which to calculate the applied potentials E_1 and E_2 (see equations (2) and (3)).

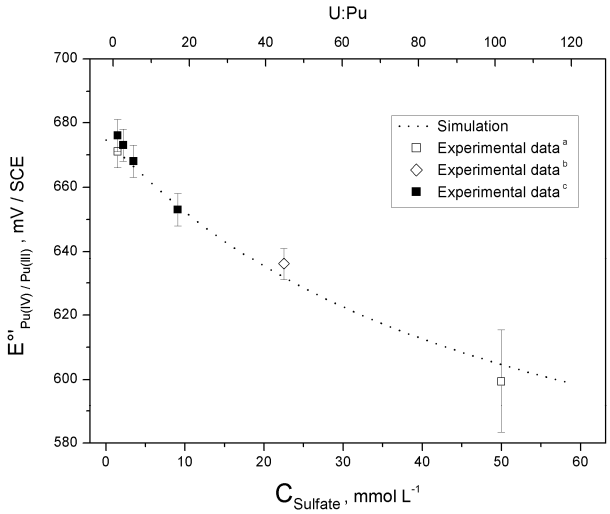

Figure 5: *Simulated (dotted line) and experimental $E^{0\prime}_{Pu(III)/Pu(IV)}$ values for Pu + U (squares) and Pu H_2SO_4 (diamonds) solutions in relation to the total $C_{sulfate}$ in solution. [a] Experimental values determined in the present study for Pu + U solutions. [b] Experimental value determined in the present study for Pu + H_2SO_4 solutions. [c] Experimental values taken from Ruas et al.*[11] *The U:Pu ratio shown as the ordinate axis at the top of the graph does not correspond to the Pu + H_2SO_4 solution. The error bars on the experimental data correspond to the expanded uncertainty (k=2, for the Pu and Pu + Pu H_2SO_4 solutions) or two times the standard deviation (for the Pu + U solutions)*

In the case of the highly accurate coulometric analysis of Pu in Pu + U solutions, the cathodic shift in $E^{0\prime}_{Pu(IV)/Pu(III)}$ induced by the complexation of sulfates is particularly important as it will significantly affect the degree of completion of the electrochemical reactions performed and therefore the importance of the f parameter (and, as such, the trueness of the analyses).

3 – Coulometry analysis

As previously shown in equation (6), during coulometric analyses the degree of completion of the electrochemical reactions is incorporated into Faraday's law by means of the "electrolysed fraction" factor, f, defined in equation (7). This factor serves two purposes: firstly, it compensates for the fact that, at the applied potentials, the performed reactions do not reach 100% completion. Secondly, it takes into account differences in reaction completion caused by the shift of the Pu(IV)/Pu(III) formal potential due to sulfate complexation.

The E_1 and E_2 potentials applied during coulometry are centred on $E^{0\prime}_{app.}$ (chosen due to its proximity to the $E^{0\prime}_{Pu(IV)/Pu(III)}$ for the pure Pu solutions in HNO_3) in order to ensure an equivalent degree of completion of the Pu oxidation and reduction reactions in media without significant sulfate complexation effects. As such, the cathodic shifts in $E^{0\prime}_{Pu(IV)/Pu(III)}$ caused by the complexation of sulfates will induce a decrease in the degree of completion of the reduction reaction and an increase in the degree of completion of the oxidation reaction. This effect is illustrated in figure 6 where the values of E_1 and E_2 determined by using $E^{0\prime}_{app.}$ as a centre point are shown in relation to the formal potentials of the three solutions studied as well as the values of E_1 and E_2 adjusted to take into account sulfate complexation in Pu + U solutions (with a centre point at 601 mV / SCE).

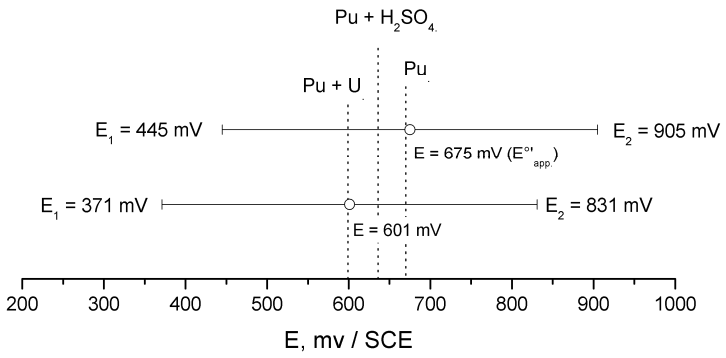

Figure 6: *$E^{0\prime}_{Pu(IV)/Pu(III)}$ of the three solutions studied (dotted lines) in relation to the position of the applied potentials E_1 and E_2 when they are determined based on $E^{0\prime}_{app.}$ (675 mV / SCE). Also shown is the case when E_1 and E_2 are adjusted to consider the complexation effects of sulfate anions from* a centre point *potential of 601 mV / SCE.*

These changes in reaction completion as caused by the differences between $E^{0\prime}_{app.}$ and the $E^{0\prime}_{Pu(IV)/Pu(III)}$ of a solution (defined as $\Delta E^{0\prime}$) will have a significant effect on the f factor. A graphical representation of this effect can be seen in the supporting information for this paper (Appendix A, section A.6, figure A.7) where formal redox potentials of the three different types of solution studied in the present experiment are reported (in terms of $E^{0\prime}_{app.}$ = 675 mV / SCE).

In situations where $\Delta E^{0\prime}$ is ≤ 10 mV, the variations in f are minute (- 0.0016%). Such cases can be seen in the present study for the analysis of pure Pu solutions (where $E^{0\prime}_{app.}$ = 675 mV / SCE and $E^{0\prime}_{Pu(IV)/Pu(III)}$ = 670 mV / SCE) and are encountered during the routine applications of coulometry for the analysis of Pu, where studied solutions remain relatively similar to each other (and thus display very small variations in $E^{0\prime}_{Pu(IV)/Pu(III)}$) [11,15]. The small variation of f in such cases signifies that the $E^{0\prime}_{Pu(IV)/Pu(III)}$ of the studied systems does not necessarily need to be measured individually for each sample in order to retain a high analytical accuracy.

However, in situations where $\Delta E^{0\prime}$ is larger, the variation of the f factor becomes more important such that at $\Delta E^{0\prime}$ values of 39 mV a variation of - 0.04% occurs in the f factor. Such a case was encountered in the present study during the analyses of Pu + H_2SO_4 solutions where $E^{0\prime}_{app.}$ = 675 mV / SCE and $E^{0\prime}_{Pu(IV)/Pu(III)}$ = 636 mV / SCE due to the increased complexation of the Pu^{4+} cations by SO_4^{2-} anions.

This effect becomes further pronounced as $\Delta E^{0\prime}$ increases. In the present experiment, $\Delta E^{0\prime}$ values of 76 mV were observed during the analyses of the Pu + U solutions ($E^{0\prime}_{app.}$ = 675 mV / SCE and $E^{0\prime}_{Pu(IV)/Pu(III)}$ = 599 mV / SCE), leading to large variations in f values (- 0.22%). Considering the importance of this variation in f values, the changes in $E^{0'}_{\mathrm{Pu(III)/Pu(IV)}}$ between the studied samples were considered non-negligible in order to perform the CPC analysis of Pu in Pu + H_2SO_4 solutions at the desired levels of accuracy in the present experiment. Experimentally, this resulted in a systematic measurement of $E^{0'}_{\mathrm{Pu(IV)/Pu(III)}}$ for each analysed sample.

It follows that, for analyses such as those performed in the present experiment, where the studied solutions have an unknown $E^{0\prime}_{Pu(IV)/Pu(III)}$ (which, in order to maintain CPC's high level of accuracy, can only be measured after performing the coulometric analysis of the sample), a systematic measurement of the analysed solutions' $E^{0\prime}_{Pu(IV)/Pu(III)}$ is essential. Such a measurement allows an accurate calculation of the f factor to compensate for each experiment's ΔE°'. In the present study the $E^{0\prime}_{\mathrm{Pu(IV)/Pu(III)}}$ of each studied solution was measured following CPC analysis, in order to adequately adjust the *f* factor to any variation in formal potential, and thereby minimise uncertainty of the results.

The collated results and key parameters for the coulometric analyses of Pu + U solutions performed in the present study are reported in table 4 in comparison to the results for pure Pu solutions as previously reported by our group [15] (the raw experimental data can be found in the supporting information in this document in section A.7 of appendix A). It can be seen that the mean Pu concentration in the analysed Pu + U samples was determined to be (1.1192 ± 0.0023) mg g^{-1} (k=2) which corresponds to a bias of less than 0.04% relative to the known reference concentration. The uncertainty on the result corresponds to 0.10 % (k=1), a value consistent with that previously reported for the analysis of pure Pu samples with five replicates (0.09%; k=1) [15]. It is thus clear that by using the f factor to take into account the shifts in $E^{0\prime}_{Pu(III)/Pu(IV)}$ caused by the complexation of sulfates with Pu cations, it was possible to reach a good degree of analytical accuracy even in the presence of large amounts of U (and consequently SO_4^{2-}).

Furthermore, it is important to note that this study's results are in good agreement with the international atomic energy agency's (IAEA) international target values (ITVs-2010) of 0.14% (k=1)

[10]. This coherence between uncertainties demonstrates that coulometry can be extended effectively to the study of Pu in Pu + U solutions whilst retaining its characteristically high accuracy.

Table 4: *Collated results of the CPC analyses performed on the Pu + U solutions studied. The errors correspond to the expanded uncertainty for the values at k=2.*

Solution	$E^{0\prime}_{Pu(III)/Pu(IV)}$	f	[Pu] (mg g^{-1})	[Pu]$_{ref}$ (mg g^{-1})	Bias (%)	Source
Pure Pu	670 ± 5 [a]	0.999734 [a]	5.5307± 0.0045 [a]	5.5326± 0.0066 [a]	-0.03 [a]	Picart *et al.* [a]
Pu + U	600 ± 8 [b]	0.997213 [b]	1.1192 ± 0.0023 [b]	1.1192 ± 0.0066 [b]	Less than 0.04 [b]	Present study

[a] *The results for this series correspond to the arithmetic mean of 5 samples, taken from Picart et al.*[15]

[b] *The values for this series correspond to the arithmetic mean of 8 samples analysed in the present experiment.*

A deeper understanding on the precision of the coulometric procedures, as well as the effects of varying the E_1 and E_2 applied potentials, can be gained by studying individual analysis results. Table 5 compares the CPC analysis results of four samples originating from a given Pu + U standard solution (vial #S061, U:Pu = 95.6) analysed using E_1 and E_2 determined by using $E^{0\prime}_{app.}$ as a centre point, with the results of four samples of another Pu + U standard solution (vial #S089, U:Pu = 95.6) where E_1 *and* E_2 are based on a centre point of 601 mV / SCE. The bias of the CPC analyses of Pu + U solutions relative to the known reference concentration of Pu in the solutions is also shown in figure 7 for clarity.

From the first series of results presented in table 5 and figure 7, it was possible to investigate the accuracy of the applied experimental protocol. The relative standard deviation between the results of samples YD 48, YD 49, YD50, and YD 51 was calculated to be 0.17% (corresponding to a standard deviation of 0.00095 mg g^{-1} of Pu).

A better estimate of the CPC measurement uncertainty was achieved by applying the Monte Carlo Method of statistical analysis previously described by Picart *et al.*[15] (an example of this calculation is provided in this paper's supporting information, appendix A, section A.8). Through this method, a standard uncertainty of 0.00078 mg g^{-1} was estimated for the CPC analyses performed in the present study. From this uncertainty value as well as the relative standard deviation between the results, the coulometric procedure used for the analysis of mixed Pu + U solutions during this experiment can be seen to display a good precision.

The significance of the bias reported in table 5 (-0.014%) for the analyses YD48 to YD51 can be analysed through the use of the normalised deviation term, E_n, as previously described by Picart *et al.*[15] E_n can be calculated as shown in equation (18), where u_{exp} and u_{ref} are the standard uncertainties on the studied sample's mean experimental Pu content and reference Pu content values, respectively. If the E_n for a given set of data is less than 2 in absolute terms, the bias in the method is considered non-significant. In the case of the present experiment, the E_n for a mean of five replicate CPC analyses of Pu + U solutions is 0.14. As the calculated E_n value is inferior to 2, the bias of

the analyses can be considered non-significant. It follows that, when using the procedure presented in this study, the CPC analysis can be considered a true method for Pu amount determination in presence of U.

$$E_n = \frac{\left|[Pu]_{mean} - [Pu]_{ref}\right|}{\sqrt{u_{exp}^2 - u_{ref}^2}} = \frac{|1.11904 - 1.11920|}{\sqrt{0.00095^{\,2} - 0.00046^{\,2}}} = 0.14 \qquad (18)$$

The final result for this series of analyses can thus be expressed from the mean value of the 4 replicates and the expanded uncertainty calculated by the Monte Carlo Method as:

[Pu] = (1.11904 ± 0.00155) mg g^{-1} with a relative expanded uncertainty of 0.14% (k=2).

It is important to note that the results for experiments YD48 to YD 51 (seen in table 5) were obtained from coulometric analyses where the applied potentials E_1 and E_2 were determined from $E^{0\prime}_{app.}$ (which differs by circa 75 mV from the $E^{0\prime}_{Pu(IV)/Pu(III)}$ of the studied Pu + U solutions). As seen in figure 6, this shift resulted in $E^{0\prime}_{Pu(IV)/Pu(III)}$ no longer being centred between E_1 and E_2 . Indeed the applied E_1 was then only distant by 160 mV from the solution's $E^{0\prime}_{Pu(IV)/Pu(III)}$ (consequently, the oxidizing potential E_2 was 300 mV from the solution's $E^{0\prime}_{Pu(IV)/Pu(III)}$). This shift induced a change of more than 0.1% in the completion of the first electrochemical step performed during CPC analysis, explaining the large variation observed in f (shown in figure A.7 (Appendix A, section A.6)). Nonetheless, the good precision in reproducibility conditions (table 5) as well as the high accuracy (table 4) of the results obtained demonstrate the suitability of f as a corrective factor during coulometric analysis.

Table 5: *CPC analysis results of Pu + U solutions (U:Pu = 95.6) when E_1 and E_2 were determined from $E^{0\prime}_{app.}$ in comparison to the results obtained when E_1 and E_2 were adjusted to take into account sulfate complexation.*

Experiment ID	E_1 (mV / SCE)	E_2 (mV / SCE)	$E^{0\prime}_{Pu(III)/Pu(IV)}$ (mV / SCE)	f	[Pu] (mg g^{-1})	$[Pu]_{ref}$ (mg g^{-1})	Bias (%)
YD 48	445	905	620	0.9988917	1.1189	1.1192	-0.026
YD 49			602	0.9977704	1.1199	1.1192	0.061
YD 50			592	0.9967339	1.1165	1.1192	-0.243
YD 51			595	0.9971333	1.1209	1.1192	0.151
			Mean [Pu] (mg g^{-1})		1.1190	**Mean bias (%)**	-0.014
			[Pu] RSD (%)		0.17		
YD 56	371	831	591	0.9997337	1.1219	1.1192	0.245
YD 57			593	0.9997387	1.1170	1.1192	-0.194
YD 58			600	0.9997365	1.1188	1.1192	-0.034
YD 59			602	0.999745	1.1199	1.1192	0.064

Mean [Pu] (mg g^{-1})	1.1194	**Mean bias (%)**	0.018
[Pu] RSD (%)	0.184		

Once the $E^{0'}_{\mathrm{Pu(IV)/Pu(III)}}$ of the Pu +U solution is known, it is possible to shift E_1 and E_2 to accommodate for the change in $E^{0'}_{\mathrm{Pu(IV)/Pu(III)}}$ induced by the sulfate complexation. The shifted potential, set to 601 mV / SCE, can be seen in figure 6. This shift recentres E_1 and E_2 around the $E^{0\prime}_{\mathrm{Pu(IV)/Pu(III)}}$ of the Pu + U solutions, thereby enabling a more complete reduction during the first step of CPC analysis. The effect of adapting the potentials applied during CPC analysis to compensate for the shift in $E^{0'}_{\mathrm{Pu(IV)/Pu(III)}}$ can be seen in the second set of results reported in table 5 and figure 7, where E_1 and E_2 were adjusted to have a centre point at 601 mV / SCE. It is also important to note that the shift in potentials changes the value of f from 0.9976 to 0.9997, thus reducing its impact on the overall analysis result.

For this second series of analyses, an average bias of 0.018% and a relative standard deviation of 0.18% (corresponding to an absolute uncertainty of 0.0010 mg g^{-1} of Pu) were calculated. The E_n for this series of results was thus calculated to be 0.16, demonstrating the non-significance of the bias. As such, it was possible to express the final results for this series of experiments through the mean value of the 4 replicates and the expanded uncertainty calculated by the Monte Carlo Method:

[Pu] = (1.11939 ± 0.00155) mg g^{-1} with a relative expanded uncertainty of 0.14% (k=2).

By comparing the two sets of data in table 5 and figure 7, it can be seen that whilst adapting the applied potentials to the solution's $E^{0\prime}_{Pu(IV)/Pu(III)}$ decreased the significance of the f factor (bringing it closer to 1), it did not significantly increase the accuracy of the final analysis results. In fact, the analyses performed by using shifted E_1 and E_2 values showed a non-significantly different accuracy (trueness: average bias of 0.018%) and precision (RSD of 0.18%) with respect to those performed whilst applying the unadjusted E_1 and E_2 potentials (trueness: bias of -0.014 % and precision: RSD of 0.17%). Consequently, as can be seen in figure 7, as long as a studied solution's $E^{0'}_{\mathrm{Pu(IV)/Pu(III)}}$ is appropriately determined in order to calculate the f factor, shifting the E_1 and E_2 potentials during CPC analysis does not bring significant advantages. Furthermore, it is important to remember that, in order to achieve a high analytical accuracy during CPC, the deviation between $E^{0\prime}_{app.}$ and $E^{0\prime}_{Pu(IV)/Pu(III)}$ must be taken into account, rendering the measurement of the studied solution's $E^{0\prime}_{Pu(IV)/Pu(III)}$ imperative.

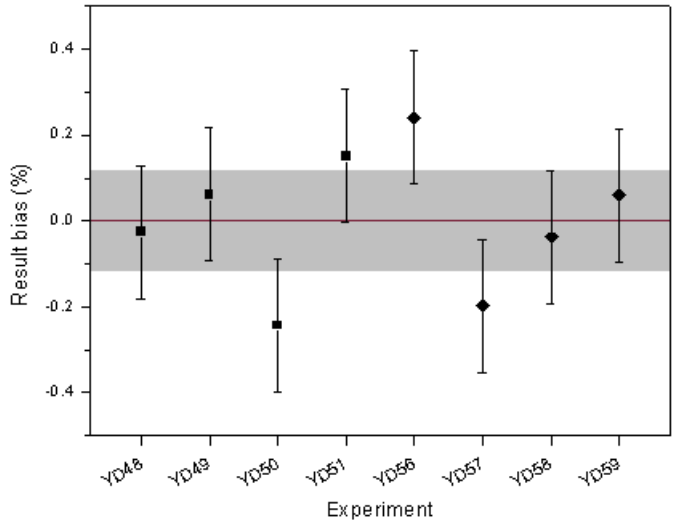

Figure 7: *Bias of the CPC analysis results for experiments YD48-51 (squares) and YD56-59 (diamonds), the grey band corresponds to the 0.12% uncertainty on the reference Pu concentrations.*

Based on the results hitherto obtained, the authors of this paper recommend that, when performing CPC analyses of Pu on mixed Pu + U solutions (or, in a more general term, CPC analyses of solutions wherein the formal potential of the studied redox couple is shifted from a known value of apparent potential), the $E^{0\prime}_{Pu(IV)/Pu(III)}$ of the studied solutions should be measured systematically for each solution. Such a measurement, performed through the use of a coulogram only after CPC analysis, would allow to calculate an appropriate f factor for the studied systems. Finally, whilst it is possible to implement a shift in applied potentials to compensate for variations in formal potential in the case of sulfate complexation, this does not provide an improvement in analysis results.

Conclusions

During the series of experiments presented in this paper, it was shown that the coulometric determination of Pu can be applied to mixed Pu + U nitric acid solutions containing large quantities of U (U:Pu ≤ 95.6) whilst maintaining the technique's particularly high accuracy. Indeed, the uncertainty of the CPC analysis performed on Pu + U nitric acid solutions (0.08% at k=1) was consistent with IAEA's ITVs-2010 values for the CPC analysis of Pu in Pu nitric acid solutions (0.14% at k=1) [10]. These results demonstrate the applicability of CPC, as performed with the procedure detailed in this study, for the routine analysis of mixed Pu + U solutions at an international level.

The in-depth electrochemical studies performed further allowed attribution of the interferences previously observed by Ruas et al. during the CPC analysis of Pu in Pu + U solutions to the presence of sulfate ions introduced with the U as UO_2SO_4 crystals in the fuming step. The particular role of the sulfate ions was further explored through speciation simulation studies, which demonstrated a preferential complexation of the SO_4^{2-} anions towards Pu^{4+} rather than Pu^{3+} cations in solution and allowed to quantify the effect of this complexation on the decrease of the formal potential of the Pu(IV)/Pu(III) redox couple. The difference between the complexation of Pu(IV) and Pu(III) leads to a shift in $E^{0\prime}_{Pu(III)/Pu(IV)}$ between pure Pu solutions and mixed Pu + U solutions, which affects the degree of completion of the electrochemical reactions performed during CPC analysis. In the present

experiment, it was shown that the corrective "electrolysed fraction" factor, f, which is usually applied in order to reach a high analytical accuracy, was also effective in compensating for the shifts in $E^{0\prime}_{Pu(III)/Pu(IV)}$ arising from the complexation of sulfates. Although the importance of f on the analysis results increased as the $E^{0\prime}_{Pu(III)/Pu(IV)}$ drifted from that of pure Pu nitrate solutions, the accuracy of the CPC analyses remained unaffected.

Ultimately, it was possible to establish recommendations for the high accuracy CPC analysis of Pu in the presence of large quantities of U (U:Pu ratios up to 95.6:1). These recommendations, as well as the increased understanding of the speciation of Pu in Pu + U aqueous acidic solutions in relation to sulfates in an HNO_3 medium, will be particularly important for the future adoption of CPC as a cornerstone in the metrology of Pu in mixed Pu + U solutions.

Acknowledgments

The authors would like to thank Denis Roussignol and Estelle Machon from the Analysis Laboratory of the ATALANTE facility (L2AT) for the sulfate content analyses of the solutions studied in this experiment.

The authors are further thankful to Thomas Charles Draper from Harvard university for his proofreading and advice during the writing of this text.

We would like also to acknowledge Laurence Bonnet (CEA defence and security research directorate), Catherine Bergé-Thierry (CEA international relations directorate), Emmanuel Touron and Andrea Salvatores (CEA low carbon energies directorate) for their financial support.

Bibliography

[1] International Energy Agency, World Energy Outlook 2019, OECD Publishing, Paris, 2019. https://doi.org/10.1787/caf32f3b-en.

[2] Euratom, Supply Agency, Euratom Supply Agency annual report 2018., 2019. http://publications.europa.eu/publication/manifestation_identifier/PUB_MJAA19001ENN (accessed April 27, 2020).

[3] C. Poinssot, C. Rostaing, S. Greandjean, B. Boullis, Recycling the Actinides, The Cornerstone of Any Sustainable Nuclear Fuel Cycles, Procedia Chem. 7 (2012) 349–357. https://doi.org/10.1016/j.proche.2012.10.055.

[4] M. Crozet, D. Roudil, C. Rigaux, C. Bertorello, S. Picart, C. Maillard, EQRAIN: uranium and plutonium interlaboratory exercises from 1997 to 2016—comparison to ITVs-2010, J. Radioanal. Nucl. Chem. 319 (2019) 1013–1021. https://doi.org/10.1007/s10967-018-6399-7.

[5] Z. Varga, C. Venchiarutti, A. Nicholl, J. Krajkó, R. Jakopič, K. Mayer, S. Richter, Y. Aregbe, IRMM-1000a and IRMM-1000b uranium reference materials certified for the production date. Part I: methodology, preparation and target characteristics, J. Radioanal. Nucl. Chem. 307 (2016) 1077–1085. https://doi.org/10.1007/s10967-015-4227-x.

[6] A. Shakhashiro, S. Tarjan, A. Ceccatelli, G. Kis-Benedek, M. Betti, IAEA-447: A new certified reference material for environmental radioactivity measurements, Appl. Radiat. Isot. 70 (2012) 1632–1643. https://doi.org/10.1016/j.apradiso.2012.03.024.

[7] C. Rivier, D. Roudil, C. Rigaux, B. Camès, J.M. Adnet, C. Eysseric, B. Tufféry, A. Ruas, C. Lamouroux, F. Casanova, M. Organista, P. Pochon, Validation of analytical methods for nuclear spent fuel reprocessing, Prog. Nucl. Energy. 72 (2014) 115–118. https://doi.org/10.1016/j.pnucene.2013.07.017.

[8] C. Rivier, M. Désenfant, M. Crozet, C. Rigaux, D. Roudil, B. Tufféry, A. Ruas, Use of an excess variance approach for the certification of reference materials by interlaboratory comparison, Accreditation Qual. Assur. 19 (2014) 269–274. https://doi.org/10.1007/s00769-014-1066-3.
[9] D. Roudil, C. Rigaux, C. Rivier, J.C. Hubinois, L. Aufore, CETAMA Contribution to Safeguards and Nuclear Forensic Analysis based on Nuclear Reference Materials, Procedia Chem. 7 (2012) 709–715. https://doi.org/10.1016/j.proche.2012.10.108.
[10] K. Zhao, M. Penkin, C. Norman, S. Balsley, K. Mayer, P. Peerani, C. Pietri, S. Tapodi, Y. Tsutaki, M. Boella, G. Renha Jr, E. Kuhn, International Target Values 2010 for Measurement Uncertainties in Safeguarding Nuclear Materials - report number IAEA-STR-368, IAEA, International Atomic Energy Agency (IAEA), Vienna (Austria), 2010. https://esarda.jrc.ec.europa.eu/images//Bulletin/Files/B_2012_048.pdf.
[11] A. Ruas, N. Leguay, R. Sueur, N. Vedel, V. Dalier, P. Moisy, High accuracy plutonium mass determination by controlled-potential coulometry, Radiochim. Acta. 102 (2014) 691–699. https://doi.org/10.1515/ract-2013-2213.
[12] V.N. Momotov, E.A. Erin, Coulometric methods for uranium and plutonium determination, Radiochemistry. 59 (2017) 1–25. https://doi.org/10.1134/S1066362217010015.
[13] A. Macdonald, D.J. Savage, Plutonium accountancy in reprocessing plants by ceric oxidation, ferrous reduction and dichromate titration. - report number IAEA-AM-231/52, IAEA, 1979.
[14] D.B. Newell, F. Cabiati, J. Fischer, K. Fujii, S.G. Karshenboim, H.S. Margolis, E. de Mirandés, P.J. Mohr, F. Nez, K. Pachucki, T.J. Quinn, B.N. Taylor, M. Wang, B.M. Wood, Z. Zhang, The CODATA 2017 values of h , e , k , and N_A for the revision of the SI, Metrologia. 55 (2018) L13–L16. https://doi.org/10.1088/1681-7575/aa950a.
[15] S. Picart, M. Crozet, G. Canciani, Y. Davrain, L. Faure, D. Roudil, Accurate determination of plutonium by Controlled Potential Coulometry: uncertainty evaluation by the Monte Carlo Method approach, J. Radioanal. Nucl. Chem. 324 (2020) 747–758. https://doi.org/10.1007/s10967-020-07085-w.
[16] S. Kihara, Z. Yoshida, H. Aoyagi, K. Maeda, O. Shirai, Y. Kitatsuji, Y. Yoshida, A Critical Evaluation of the Redox Properties of Uranium, Neptunium and Plutonium Ions in Acidic Aqueous Solutions, Pure Appl. Chem. 71 (1999) 1771–1807. https://doi.org/10.1351/pac199971091771.
[17] W. Shults, Applications of controlled-potential coulometry to the determination of plutonium, Talanta. 10 (1963) 833–849. https://doi.org/10.1016/0039-9140(63)80244-1.
[18] S. Georgette, Réduction cathodique de solutions mixtes uranium/plutonium en milieu acide nitrique dans un électrolyseur plaque en présence d'un agent anti-nitreux, Université de Lorraine, 2014. http://www.theses.fr/2014LORR0214.
[19] F.A. Scott, R.M. Peekema, Analysis for Plutonium by Controlled-potential Coulometry, in: Proc. Second U. N. Int. Conf. Peac. Uses At. Energy, United Nations, Geneva, 1958: pp. 573–578.
[20] Y. Duigou, W. Leidert, A test for the reliability of the controlled potential coulometric method to determine plutonium in uranium-plutonium mixtures, Fresenius Z. Für Anal. Chem. 279 (1976) 29–32. https://doi.org/10.1007/BF00424235.
[21] Y. Duigou, W. Leidert, Influence of a photochemical reaction on the controlled potential coulometric determination of plutonium in a mixture with uranium, Fresenius Z. Für Anal. Chem. 278 (1976) 29–31. https://doi.org/10.1007/BF00445816.
[22] J. Fardon, Controlled potential coulometry: the application of a secondary reaction to the determination of plutonium and uranium at a solid electrode, Talanta. 19 (1972) 1321–1334. https://doi.org/10.1016/0039-9140(72)80129-2.
[23] L.M. Angeletti, W.J. Bartscher, M.J. Maurice, Controlled potential coulometric determination of plutonium and uranium using a mercury pool electrode: Application to the analysis of high-fired uranium-plutonium mixed oxides, Fresenius Z. Für Anal. Chem. 246 (1969) 297–302. https://doi.org/10.1007/BF00463382.

[24] H. Takeishi, H. Muto, H. Aoyagi, T. Adachi, K. Izawa, Z. Yoshida, H. Kawamura, S. Kihara, Determination of oxygen/uranium ratio in irradiated uranium dioxide based on dissolution with strong phosphoric acid, Anal. Chem. 58 (1986) 458–462. https://doi.org/10.1021/ac00293a043.
[25] J.E. Rein, G.M. Matlack, G.R. Waterbury, R.T. Phelps, C.F. Metz, Methods of Chemical Analysis for FBR Uranium-Plutonium Oxide Fuel and Source Materials, Los Alamos Scientific Laboratory, 1971.
[26] F. Scholz, A.M. Bond, R.G. Compton, D.A. Fiedler, G. Inzelt, H. Kahlert, š. Komorsky-Lovrić, H. Lohse, M. Lovrić, F. Marken, A. Neudeck, U. Retter, F. Scholz, Z. Stojek, eds., Electroanalytical Methods, Springer Berlin Heidelberg, Berlin, Heidelberg, 2010. https://doi.org/10.1007/978-3-642-02915-8.
[27] G.C. Goode, J. Herrington, High-speed controlled-potential coulometry, Anal. Chim. Acta. 33 (1965) 413–417. https://doi.org/10.1016/S0003-2670(01)84912-6.
[28] J.J. Carbajo, G.L. Yoder, S.G. Popov, V.K. Ivanov, A review of the thermophysical properties of MOX and UO2 fuels, J. Nucl. Mater. 299 (2001) 181–198. https://doi.org/10.1016/S0022-3115(01)00692-4.
[29] C. Maillard, J.-M. Adnet, Plutonium(IV) peroxide formation in nitric medium and kinetics Pu(VI) reduction by hydrogen peroxide, Radiochim. Acta. 89 (2001). https://doi.org/10.1524/ract.2001.89.8.485.
[30] P.V. Balakrishnan, A.S. Ghosh Mazumdar, Observations on the action of hydrogen peroxide on trivalent and tetravalent plutonium solutions, J. Inorg. Nucl. Chem. 26 (1964) 759–765. https://doi.org/10.1016/0022-1902(64)80320-1.
[31] Controlled-potential coulometric assay of plutonium, ISO 12183:2018, 2018.
[32] C26 Committee, Test Method for Plutonium by Controlled-Potential Coulometry, ASTM International, n.d. https://doi.org/10.1520/C1108-99.
[33] A. Fallet, N. Larabi-Gruet, S. Jakab-Costenoble, P. Moisy, Electrochemical behavior of plutonium in nitric acid media, J. Radioanal. Nucl. Chem. 308 (2016) 587–598. https://doi.org/10.1007/s10967-015-4423-8.
[34] M.K. Holland, J.R. Weiss, C.E. Pietri, Controlled-potential coulometric determination of plutonium, Anal. Chem. 50 (1978) 236–240. https://doi.org/10.1021/ac50024a018.
[35] I. Grenthe, F. Mompean, K. Spahiu, H. Wanner, TDB-2 Guidelines for the extrapolation to zero ionic strength, Version of 18 June 2013, Nuclear Energy Agency, Organisation for Economic Co-operation and Development, Paris, 2013.
[36] I. Grenthe, I. Puigdomenech, B. Allard, OECD Nuclear Energy Agency, eds., Estimation of Medium Effects on Thermodynamic Data, in: Model. Aquat. Chem., Nuclear Energy Agency, Organisation for Economic Co-operation and Development, Paris, 1997: pp. 325–426.
[37] A. Paulenova, G.F. Vandegrift, III, K.R. Czerwinski, Plutonium Chemistry in the UREX+ Separation Processes, Oregon State University, United States, 2009.
[38] D. Vopálka, K. Štamberg, A. Motl, B. Drtinová, The study of the speciation of uranyl–sulphate complexes by UV–Vis absorption spectra decomposition, J. Radioanal. Nucl. Chem. 286 (2010) 681–686. https://doi.org/10.1007/s10967-010-0764-5.
[39] K.L. Nash, J.M. Cleveland, Stability Constants, Enthalpies, and Entropies of Plutonium(III) and Plutonium(IV) Sulfate Complexes, in: W.T. Carnall, G.R. Choppin (Eds.), Plutonium Chem., American Chemical Society, WASHINGTON, D.C., 1983: pp. 251–262. https://doi.org/10.1021/bk-1983-0216.ch017.
[40] Y.X. Xia, J.I. Friese, D.A. Moore, P.P. Bachelor, L. Rao, Complexation of plutonium(IV) with sulfate at variable temperatures, J. Radioanal. Nucl. Chem. 274 (2007) 79–86. https://doi.org/10.1007/s10967-006-6907-z.
[41] C.D. Alcorn, J.S. Cox, L.M.S.G.A. Applegarth, P.R. Tremaine, Investigation of Uranyl Sulfate Complexation under Hydrothermal Conditions by Quantitative Raman Spectroscopy and Density Functional Theory, J. Phys. Chem. B. 123 (2019) 7385–7409. https://doi.org/10.1021/acs.jpcb.9b01544.

[42] G. Tian, L. Rao, Spectrophotometric and calorimetric studies of U(VI) complexation with sulfate at (25 to 70)°C, J. Chem. Thermodyn. 41 (2009) 569–574. https://doi.org/10.1016/j.jct.2008.10.014.
[43] R. Guillaumont, F.J. Mompean, OECD Nuclear Energy Agency, eds., Update on the chemical thermodynamics of uranium, neptunium, plutonium, americium and technetium, Elsevier ; Nuclear Energy Agency, Organisation for Economic Co-Operation and Development, Amsterdam, 2003.
[44] I. Grenthe, H. Wanner, I. Forest, OECD Nuclear Energy Agency, eds., Chemical thermodynamics of uranium, North-Holland ; Distributors for the U.S. and Canada, Elsevier Science Pub. Co, Amsterdam, 1992.
[45] L. Ciavatta, The specific interaction theory in evaluating ionic equilibria, Ann. Chim. 70 (1980) 551.
[46] T. Vercouter, B. Amekraz, C. Moulin, E. Giffaut, P. Vitorge, Sulfate Complexation of Trivalent Lanthanides Probed by Nanoelectrospray Mass Spectrometry and Time-Resolved Laser-Induced Luminescence, Inorg. Chem. 44 (2005) 7570–7581. https://doi.org/10.1021/ic048503j.
[47] P. Tkac, A. Paulenova, G.F. Vandegrift, J.F. Krebs, Modeling of Pu(IV) Extraction from Acidic Nitrate Media by Tri- *n* -butyl Phosphate, J. Chem. Eng. Data. 54 (2009) 1967–1974. https://doi.org/10.1021/je800904t.
[48] L. Ciavatta, The Specific Interaction Theory in Equilibrium-Analysis-Some Empirical Rules for Estimating Interaction Coefficients of Metal-Ion Complexes, Ann. Chim. 80 (1990) 255–263.
[49] V. Neck, M. Altmaier, T. Fanghänel, Ion interaction (SIT) coefficients for the Th4+ ion and trace activity coefficients in NaClO4, NaNO3 and NaCl solution determined by solvent extraction with TBP, Radiochim. Acta. 94 (2006). https://doi.org/10.1524/ract.2006.94.9-11.501.
[50] S. Kumar, S.B. Koganti, Prediction of Densities of Mixed Aqueous Solutions of Electrolytes-$UO_2(NO_3)_2$, $Pu(NO_3)_4$ and Nitric Acid, J. Nucl. Sci. Technol. 34 (1997) 410–412. https://doi.org/10.1080/18811248.1997.9733682.
[51] J. Wang, Analytical electrochemistry, 3rd ed, Wiley-VCH, Hoboken, N.J, 2006.
[52] R. Gupta, K. Jayachandran, S.K. Aggarwal, Single-walled carbon nanotube (SWCNT) modified gold (Au) electrode for simultaneous determination of plutonium and uranium, RSC Adv. 3 (2013) 13491. https://doi.org/10.1039/c3ra41945b.
[53] A.V. Levanov, O.Y. Isaikina, U.D. Gurbanova, V.V. Lunin, Dissociation Constants of Perchloric and Sulfuric Acids in Aqueous Solution, J. Phys. Chem. B. 122 (2018) 6277–6286. https://doi.org/10.1021/acs.jpcb.8b01947.
[54] Y.C. Wu, D. Feng, The second dissociation constant of sulfuric acid at various temperatures by the conductometric method, J. Solut. Chem. 24 (1995) 133–144. https://doi.org/10.1007/BF00972837.

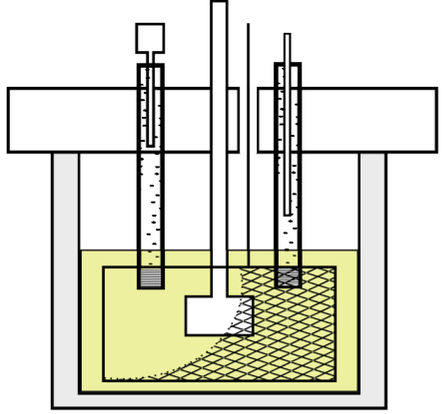

Pu
Pu + H_2SO_4 } @ HNO_3
Pu + U

Sulfate complexation

Speciation Studies

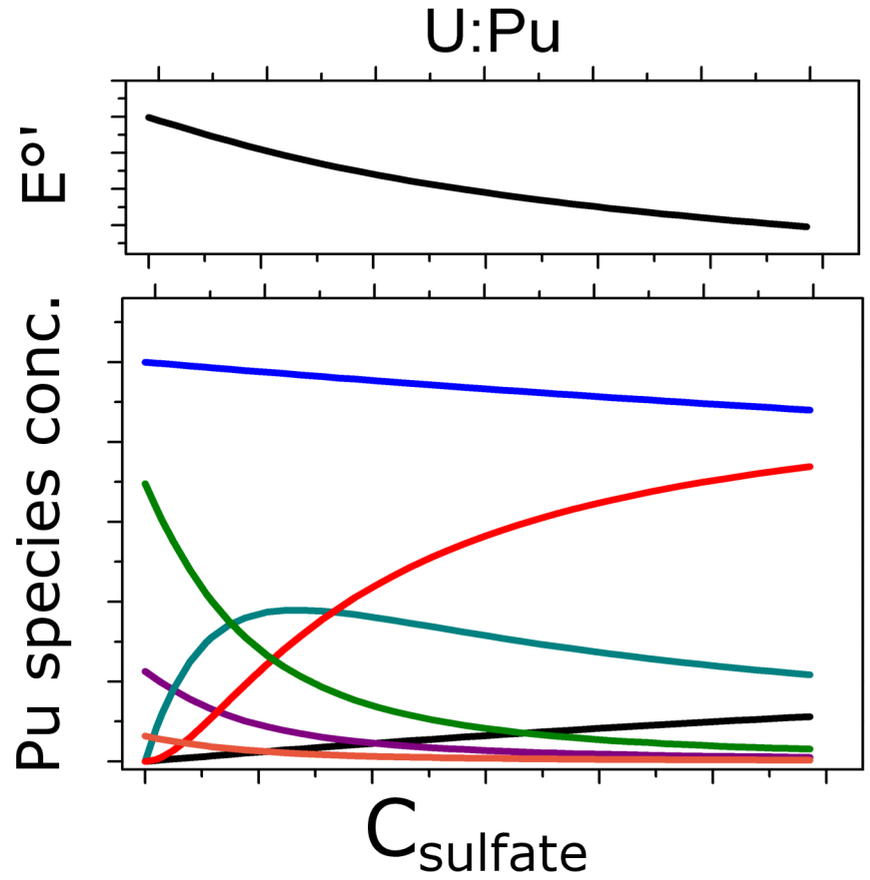

Coulometric analysis of Pu